Monatsh Chem (2010) 141:1253–1262
DOI 10.1007/s00706-010-0386-1

ORIGINAL PAPER

Synthesis and UV absorption of new conjugated quinoxaline 1,4-dioxide derivatives anticipated as tumor imaging and cytotoxic agents

Sameh R. El-Gogary · Mohamed A. Waly · Ismail T. Ibrahim · Osama Z. El-Sepelgy

Received: 1 March 2009 / Accepted: 9 August 2010 / Published online: 8 September 2010

Abstract New conjugated arylidine, enamine, and annelated pyrido derivatives of quinoxaline 1,4-dioxide were synthesized via utilization of an active allylic methyl group. Biodistribution studies were carried out by injecting a solution of an ^{125}I derivative of an enamine-substituted quinoxaline 1,4-dioxide in normal and tumor-bearing mice. The uptake in solid tumor was over 6% of the injected dose per gram tissue body weight at 4 h post injection. These data revealed localization of the tracer in the tumor tissues with a high percentage sufficient to show a radiotherapeutic effect and showed that this is a promising tool for diagnosis. Also the radiotoxicity of the ^{125}I-substituted compound on Ehrlich ascites carcinoma cells may encourage this behavior.

Keywords Quinoxaline 1,4-dioxide · Iodine-125 · Labeling · Biodistribution · Cancer

Introduction

Quinoxaline-1,4-dioxide derivatives seem to have interesting anticancer activities [1], especially in solid tumor treatment [2, 3]. Quinoxaline derivatives may act by the concept of bioreductive alkylation [4], and could cleave the DNA under hypoxic conditions in the presence of xanthine and xanthine oxidase [5]. Labeling of some quinoxaline derivatives with different radioisotopes like technetium-99 m or radioiodine was conducted for imaging or therapeutic purposes, respectively [6, 7]. Auger electron emitters are widely used in cellular radiation studies. The radiotherapeutic effectiveness of the radionuclides can be achieved by the incorporation of these radionuclides into cellular DNA leading to the breakage of the DNA double strand [8–11].

Extensive studies indicate that 3-aminoquinoxaline-2-carbonitrile 1,4-dioxide (AQCD, **2**) is more susceptible to reductive activation than tirapazamine (**1**) [12] and causes redox-activated DNA damage [13]. This was attributed to the property of **2** to absorb the radiation strongly at longer wavelengths ($\lambda_{max} \geq 350$ nm) [14]. One of the great challenges of photodynamic therapy (PDT) is to find drugs that can be activated at longer wavelengths, which in turn will increase the penetration of the tumor by photodynamic therapy [15–19]. At longer wavelengths of light, absorption by heme proteins and other reactive compounds in the blood will not interfere during therapy.

In this work, we attempted to prepare new conjugated quinoxaline 1,4-dioxide derivatives substituted at position 3 of the quinoxaline ring, which could absorb radiation at longer wavelengths (around $\lambda_{max} \geq 350$ nm). In addition, this study was conducted to find a model for labeling [(dimethylamino)vinyl]quinoxaline 1,4-dioxide (AVQD) as a vehicle to carry iodine-125 to tumor cells. In vitro radiotoxicity, in vitro stability, and in vivo biodistribution of ^{125}I-AVQD on Ehrlich ascites carcinoma (EAC) were investigated. 2-(Ethoxycarbonyl)-3-methylquinoxaline 1,4-dioxide (**3**) [20, 21], bearing an active methyl group at position 3, was selected to carry out these syntheses (Scheme 1).

S. R. El-Gogary · M. A. Waly (✉) · O. Z. El-Sepelgy
Faculty of Science (Damiatta), Chemistry Department, Mansoura University, Damiatta, Egypt
e-mail: mohamedwaly7@yahoo.com

I. T. Ibrahim
Hot Laboratories Center, Atomic Energy Authority, Cairo, Egypt

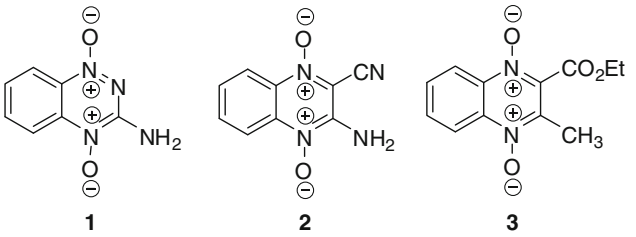

1 2 3

Scheme 1

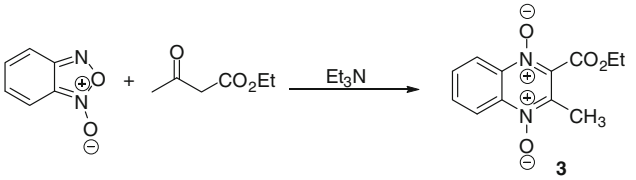

3

Scheme 2

Results and discussion

The more convenient method for the synthesis of compound **3** was the reaction of benzofurazan oxide and ethyl acetoacetate in triethylamine as a solvent and catalyst, but with a yield of only 22% [20, 21]. The amount of compound **3** was increased by a longer reaction time and an amount of ethyl acetoacetate up to 65% (Scheme 2).

Arylidine derivatives

Heating of compound **3** with an excess of aromatic aldehydes in the presence of piperidine as a catalyst gave 3-(substituted styryl)-quinoxaline 1,4-dioxide derivatives **4a**–**4e** (Scheme 3) in good yields. The structural conformation of compounds **4a**–**4e** showed that all of them are in the *trans* form, whereas their ^{1}H NMR spectra showed that the vicinal proton–proton couplings $^{3}J_{HH}$ are around 16 Hz. Also the vinylic protons appeared as double doublets in the region of $\delta = 6.76$–7.52 ppm for H_a and $\delta = 8.30$–8.38 ppm for H_b. This low field resonance value for the H_b is due to the anisotropic effect of the quinoxaline 1,4-dioxide moiety. The IR spectra for the derivatives **4** showed that the double bonds absorb in the region of 1,608–1,581 cm^{-1} in combination with aromatic absorptions. This range of absorption was attributed to the nature of substituents in the benzene ring.

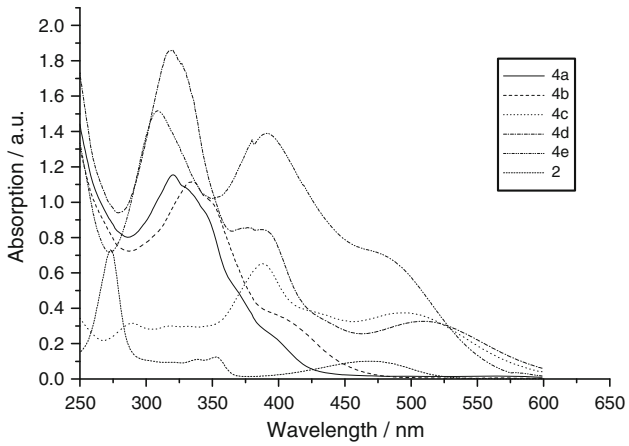

Fig. 1 Absorption spectra of arylidine derivatives **4a**–**4e** and compound **2** in methanol

Experimental UV–Vis data of arylidine derivative **4a** showed an absorption maximum at 320 nm and a weak shoulder around 400 nm. This shoulder was enhanced and developed to a peak in compounds **4b**–**4e** (Fig. 1). Furthermore, new visible absorption peaks developed at 495, 509, and 472 nm for compounds **4c**, **4d**, and **4e**, respectively (Fig. 1).

Enamine derivatives

The previous red-shift of the maximum absorptions of the arylidine derivatives **4a**–**4e** encouraged us to explore and expand this effect by formation of the enamine derivatives having similar structural features. Refluxing of compound **3** with a slight excess of dimethylformamide dimethylacetal (DMF-DMA) gave the red-colored enamine derivative **5** (AVQD, Scheme 4). The ^{1}H NMR spectrum of compound **5** shows the presence of two doublet bands at $\delta = 4.74$ (H_b) and 9.55 ppm (H_a) with a coupling constant

Scheme 3

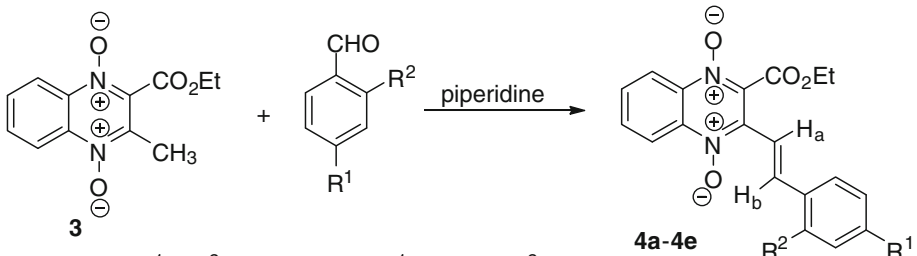

3 4a-4e

a $R^1 = R^2 = H$ **b** $R^1 = OCH_3$, $R^2 = H$
c $R^1 = NMe_2$, $R^2 = H$ **d** $R^1 = NEt_2$, $R^2 = H$
e $R^1 = NO_2$, $R^2 = OH$

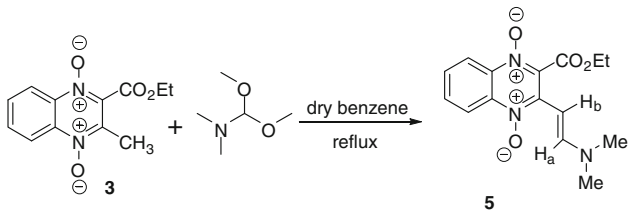

Scheme 4

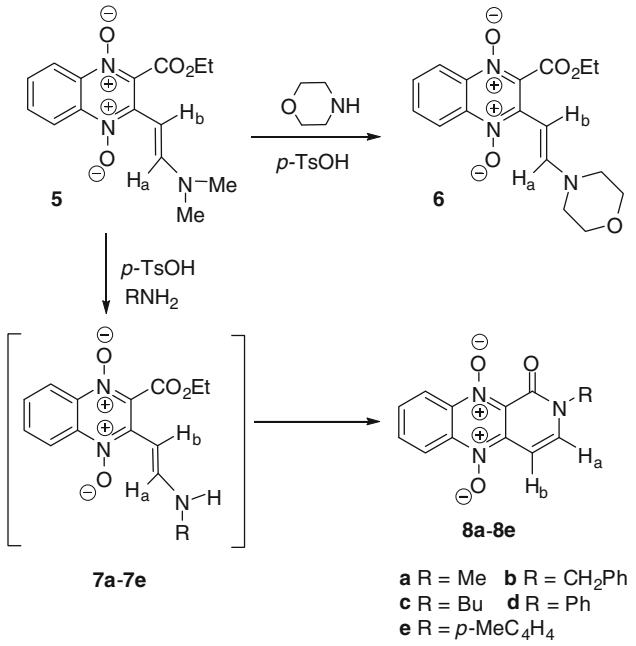

Scheme 5

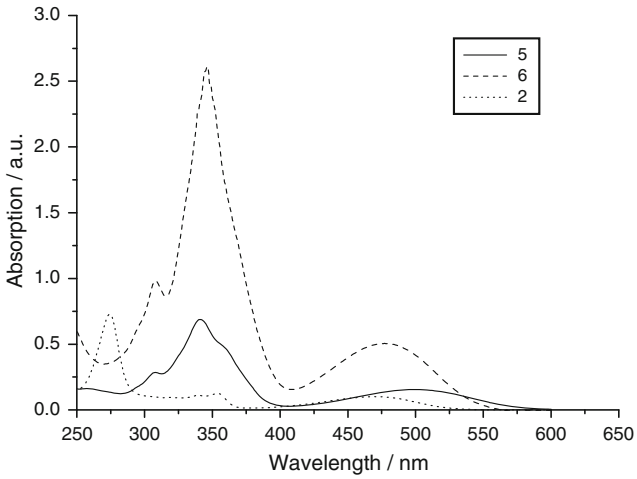

Fig. 2 Absorption spectra of **2** and **5** in methanol

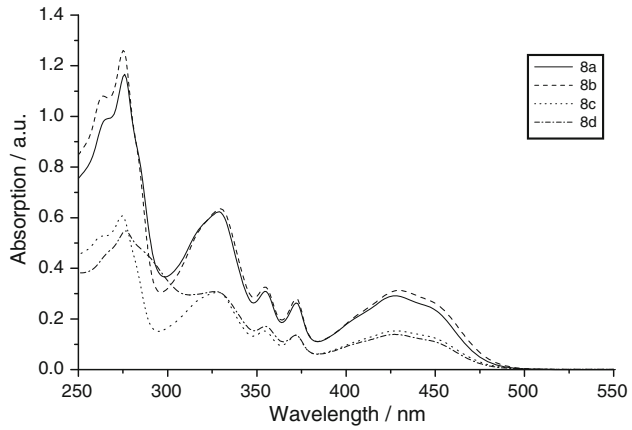

Fig. 3 Absorption spectra of **8a–8d** in methanol

of 15.5 Hz, which confirms the *trans* configuration of the double bond in enamine **5**.

Trans-amination [22] of [(dimethylamino)vinyl]quinoxaline 1,4-dioxide (AVQD) derivative **5** with secondary amines (e.g., morpholine) in the presence of *p*-toluenesulfonic acid as a catalyst afforded its morpholino-enamine analogue **6** (Scheme 5). ^{1}H NMR data for compound **6** showed the presence of two doublet bands at $\delta = 4.95$ (H_b) and 9.46 (H_a) ppm with a coupling constant of 15.3 Hz. Thus, compound **6** possesses the same configuration as its parent enamine **5** (AVQD).

Both enamine derivatives **5** and **6** have the same absorption maxima at around 350 and 500 nm, but with dramatic enhancement in absorption for **6** compared with compounds **2** and **5** (Fig. 2).

Further trans-amination reactions of the enamine derivative **5** by the same reaction conditions with primary aliphatic amines (methylamine, *n*-butylamine, and benzylamine) or aromatic amines (aniline and *p*-toluidine) gave the cyclized pyrido[3,4-*b*]quinoxaline derivatives **8a–8e** (Scheme 5). The mechanism for this cyclization might proceed through two subsequent steps. The first one includes trans-amination of compound **5** with the primary amine in the presence of *p*-toluenesulfonic acid to give inseparable secondary enamine intermediates **7a–7e**, followed by an intramolecular amidation reaction of the ester group with the enamine in the second step.

The IR spectra for these cyclized products **8a–8e** showed the presence of absorptions for the new cyclized amide carbonyl group at 1,678–1,670 cm^{-1}. The ^{1}H NMR data for **8a–8e** showed the downfield shifting for the H_b protons in this series to the aromatic proton region, while the H_a values stayed the same without changing. The coupling constants for these compounds are around $J = 9.3$ Hz, which reflects that they exist in the *cis* form. The experimental UV data for these cyclized enamine derivatives **8a–8e** (Fig. 3) did not show a significant red-shifting ($\lambda_{max} = 261$–274 nm).

Labeling of AVQD with iodine-125

^{125}I-AVQD was prepared by electrophilic substitution of H_b with iodonium ion using NBS as oxidizing agent [23]. It was reported that there are different factors that may affect labeling yield, such as: (1) oxidizing agent, (2) substrate content, (3) pH of the reaction, and (4) reaction time [24]. Thus, these parameters were carefully examined in such a way that other factors were kept at optimum conditions while the influence of one factor was studied.

Oxidizing agent content

The results obtained in this study reveal that the electrophilic substitution of the iodonium ion [$*I^+$] onto the AVQD molecule afforded a high radiochemical yield by utilizing NBS as an oxidizing agent (Table 1). It was observed that the radiochemical yield significantly increased by increasing the amount of NBS from 5 to 25 μg (optimum content) for labeling of 10 μg AVQD at which maximum labeling yield was obtained. By increasing the amount of NBS above 50 μg, the yield showed no significant change. A significant reduction in the labeling yield was noted by decreasing the concentration of NBS below 25 μg, which may be explained by the fact that at low concentrations of NBS not all iodide is converted to iodonium ions, and thus the yield is decreased in the same way as described by Yamada et al. [24].

Substrate content

The increase in the AVQD concentration was accompanied by a significant increase in the labeling yield, where it reached above 90% when 10 μg of AVQD was treated with 25 μg NBS in 250 mm^3 puffer solution. A further increase in the amount of AVQD above 10 μg did not show a significant improvement of the labeling yield. Increasing the concentration of starting material usually increases the total incorporation of radioiodine, since there is a minimum limit to the volume used [25].

Effect of pH

In order to find a suitable pH value for maximum radiochemical yield, radioiodination of AVQD was carried out at different pH ranging from 2 to 11. As shown in Table 2, pH 9 was the optimum at which the maximum yield was obtained (95.3%). The data obtained reveal very interesting and consistent findings. At lower pH (2–4) and higher pH (11), the labeling yield was significantly decreased.

Reaction time

Table 3 shows the relationship between the reaction time and the yield of ^{125}I-AVQD. Radiochemical yield was significantly increased from 89.9 to 96.3% with increasing reaction time from 1 min to 10 min. Extending the reaction

Table 1 Effect of NBS content on the radiochemical yield of ^{125}I-AVQD

NBS (μg)	% Labeled compound	% Free iodide
5	80.4 ± 0.40	19.6 ± 0.30
10	94.6 ± 0.50[a]	5.4 ± 0.25
25	97.1 ± 0.54[a,b]	2.9 ± 0.06
50	96.2 ± 0.32[a]	3.8 ± 0.31
100	96.7 ± 0.30[a]	3.3 ± 0.15

Values represent the mean ± SEM ($n = 6$)

[a] Significantly different from the initial values using unpaired Student's t test ($p < 0.05$)

[b] Significantly different from the previous values using unpaired Student's t test ($p < 0.05$)

Table 2 Effect of pH of the reaction medium on the labeling yield of ^{125}I-AVQD

pH value	% Labeled compound	% Free iodide
2	8.4 ± 0.11	91.6 ± 0.15
4	65.7 ± 0.40[a]	34.3 ± 0.60
7	85.5 ± 0.30[a,b]	14.5 ± 0.20
9	95.3 ± 0.4[a,b]	4.7 ± 0.25
11	82.0 ± 0.20[a,b]	18.0 ± 0.40

Values represent the mean ± SEM ($n = 6$)

[a] Significantly different from the initial values using unpaired Student's t test ($p < 0.05$)

[b] Significantly different from the previous values using unpaired Student's t test ($p < 0.05$)

Table 3 Effect of reaction time on the labeling yield of ^{125}I-AVQD

Time (min)	% Labeled compound	% Free iodide
1	89.9 ± 0.36	10.1 ± 0.55
5	94.1 ± 0.29[a]	5.9 ± 0.3
10	96.3 ± 0.21[a,b]	3.7 ± 0.15
15	97.2 ± 0.35[a]	2.8 ± 0.15
30	96.3 ± 0.50[a]	3.7 ± 0.15
60	96.5 ± 0.14[a]	3.5 ± 0.25

Values represent the mean ± SEM ($n = 6$)

[a] Significantly different from the initial values using unpaired Student's t test ($p < 0.05$)

[b] Significantly different from the previous values using unpaired Student's t test ($p < 0.05$)

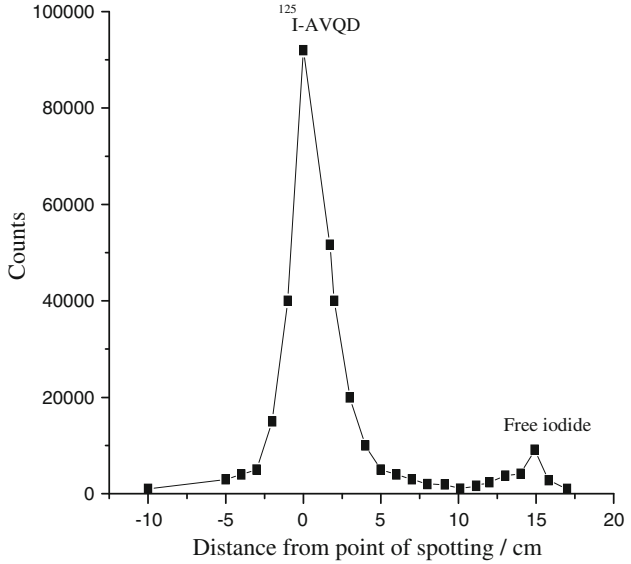

Fig. 4 Paper electrophoresis pattern of the radioiodinated ^{125}I-AVQD

time to 60 min produced no significant change of the radiochemical yield.

Electrophoresis analysis

Two main peaks were formed during the analysis of the fractions produced in the reaction by electrophoresis as illustrated in Fig. 4. The first one corresponded to free iodide that moved towards the anode with 16 cm distance at the conditions mentioned in the "Experimental" section. The second peak represented I-AVQD and stayed at the point of spotting as it was observed for ^{125}I-UdR (^{125}I-iododeoxyuridine) under the same electrophoretic conditions [23].

In vitro stability of ^{125}I-AVQD

No significant decrease in the stability of ^{125}I-AVQD up to 48 h post labeling was observed. This indicates the stability of the labeled compound.

Biodistribution of ^{125}I-AVQD

In normal mice

A biodistribution study of ^{125}I-AVQD in normal mice showed that ^{125}I-AVQD was distributed rapidly in blood, stomach, heart, and kidney at 15 min post injection. After 1 h, ^{125}I-AVQD uptake was significantly decreased in organs and tissues like blood, heart, liver, and intestine. However, ^{125}I-AVQD uptake was significantly increased in stomach, muscle, and thyroid after 1 h. At 4 h and 24 h post injection, the majority of organs and tissues showed a significant decrease in ^{125}I-AVQD uptake. The thyroid gland showed a significant increase in ^{125}I-AVQD uptake at 4 h post injection and also at 24 h when compared to each previous value (Table 4).

In solid tumor-bearing mice

Biodistribution of ^{125}I-AVQD in solid tumor-bearing mice was found to be greatest in blood, stomach, and kidney (13.3, 12.3, and 9.5%, respectively) at 15 min post injection and lowest in left leg, muscle, and thyroid (1.4, 1.2, and 0.9%, respectively; Table 5). The biodistribution of ^{125}I-AVQD in the right thigh (inoculated) was greater than in the left one. The uptake of ^{125}I-AVQD in the right thigh was significantly increased with time at 1 h and 4 h post injection, as it was 5.7 and 8.5 per gram, respectively.

The liver showed a significant decrease in ^{125}I-AVQD uptake at 1 h and 4 h post injection when compared with its previous value. In addition, ^{125}I-AVQD uptake in the

Table 4 Biodistribution of ^{125}I-AVQD in normal mice

Organs and body fluids	Percent I.D./g organ			
	Time post injection			
	15 min	1 h	4 h	24 h
Blood	21 ± 0.1	11.1 ± 0.21[a]	7.4 ± 0.04[a]	1.7 ± 0.3[a]
Bone	3.6 ± 0.05	2.1 ± 0.1[a]	1.7 ± 0.1[a]	0.7 ± 0.1[a]
Muscle	4.3 ± 0.01	5.7 ± 0.02[a]	2.6 ± 0.1	0.5 ± 0.02[a]
Liver	6.4 ± 0.05	3.3 ± 0.15[a]	3.1 ± 0.06[a]	1.0 ± 0.02
Lung	9.1 ± 0.1	4.8 ± 0.12[a]	2.9.0 ± 0.2[a]	1.0 ± 0.01[a]
Heart	9 ± 0.8	6.4 ± 0.3[a]	4.0 ± 0.01[a]	1.7 ± 0.04[a]
Stomach	22.2 ± 0.9	33.2 ± 0.6	28.6 ± 0.16[a]	12.7 ± 0.2[a]
Intestine	8.4 ± 0.50	6.1 ± 0.3[a]	4.5 ± 0.1[a]	1.5 ± 0.03[a]
Kidney	10.7 ± 0.4	8.20 ± 0.6[a]	6.6 ± 0.3[a]	3.5 ± 0.06[a]
Spleen	2.4 ± 0.3	3.3 ± 0.1[a]	3.1 ± 0.02	1.8 ± 0.05[a]
Thyroid	3.1 ± 0.02	6.6 ± 0.14[a]	8.3 ± 0.16[a]	11.2 ± 0.2[a]

Values represent mean ± SEM

[a] Means significantly differ from the previous value using unpaired Student's *t* test ($p < 0.05$)

Table 5 Biodistribution of ^{125}I-DMA in solid tumor-bearing mice

Organs and body fluids	Percent I.D./g organ			
	Time post injection			
	15 min	1 h	4 h	24 h
Blood	13.3 ± 1.8	9.1 ± 0.6[a]	4.7 ± 0.2[a]	1.2 ± 0.2[a]
Bone	2.4 ± 0.15	2.5 ± 0.1	1.4 ± 0.1[a]	1.1 ± 0.1[a]
Muscle	1.2 ± 0.15	1.5 ± 0.1	1.4 ± 0.1[a]	1.1 ± 0.1[a]
Liver	5.5 ± 0.4	3.7 ± 0.2[a]	2.1 ± 0.1[a]	0.7 ± 0.1[a]
Lung	8.1 ± 0.5	6.1 ± 0.3[a]	4 ± 0.2[a]	1.2 ± 0.15[a]
Heart	4.9 ± 0.4	3.4 ± 0.1[a]	1.7 ± 0.05[a]	0.5 ± 0.2
Stomach	12.3 ± 0.7	10.6 ± 1[a]	5.5 ± 0.5[a]	3.2 ± 0.26[a]
Intestine	2.4 ± 0.2	2.2 ± 0.1	2.1 ± 0.3	1.6 ± 0.25
Kidney	9.5 ± 0.7	6.6 ± 0.2[a]	4.5 ± 0.3[a]	2.3 ± 0.2[a]
Spleen	4.7 ± 0.5	3.2 ± 0.4[a]	2.6 ± 0.5	1.4 ± 0.25[a]
Thyroid	0.9 ± 0.2	2.4 ± 0.3[a]	4.51 ± 0.5[a]	6.4 ± 0.9[a]
Left leg	1.4 ± 0.05	1.6 ± 0.1	1.5 ± 0.1	1.2 ± 0.03[a]
Right leg	4.2 ± 0.3	5.7 ± 0.5[a]	8.5 ± 0.8[a]	8.2 ± 1.1

Values represent mean ± SEM

[a] Means significantly differ from the previous value using unpaired Student's t test ($p < 0.05$)

stomach of solid tumor mice was significantly decreased at 1 h post injection when compared to the uptake at 15 min post injection. A significant increase in the uptake of ^{125}I-AVQD in thyroid with time may be due to in vivo deiodination of ^{125}I-AVQD [26]. A significant increase in ^{125}I-AVQD uptake in the solid tumor may interfere with DNA synthesis, and hence it may be consumed more than in other sites due to the high proliferation rate in tumor sites [27].

Radiotoxicity of ^{125}I-AVQD on Ehrlich cells

In vitro radiotoxicity of ^{125}I-AVQD on Ehrlich cells was counted by calculation of the number of non-viable cells using a haemocytometer. It was observed that increasing the dose (radioactivity) of ^{125}I-AVQD produced a significant increase in the fraction of non-viable cells up to 64 kBq (Table 6). This may be explained in that the ^{125}I-AVQD may have antitumor activity.

Table 6 In vitro toxicity of ^{125}I-AVQD

Dose (kBq)	Non-viable/total cells	% Non viable cells
1	27/189	14.25 ± 03
2	36/197	18.25 ± 1.3[a]
4	47/190	24.7 ± 2.0[a,b]
8	72/240	30.3 ± 2.1[a,b]
16	84/255	33.5 ± 2.1[a,b]
64	103/250	41.0 ± 2.50[a,b]

Values represent the mean ± SEM ($n = 6$)

[a] Significantly different from the initial values using unpaired Student's t test ($p < 0.05$)

[b] Significantly different from the previous values using unpaired Student's t test ($p < 0.05$)

Conclusion

In conclusion, new conjugated arylidine and enaminoquinoxaline 1,4-dioxide derivatives were synthesized and showed UV absorptions around $\lambda_{max} \geq 350$ nm. The great incorporation of ^{125}I-AVQD in tumor sites (solid tumor) facilitates tumor imaging and could be considered an ideal vector to carry iodine-125 to the nucleus of tumor cells. This also shows the need for more studies to investigate the possibility of using ^{125}I-AVQD and similar models in the treatment of tumors.

Experimental

Thin layer and column chromatography was performed using silica gel type 60, Merck 7731 and Merck 7734, respectively. Melting points were determined on a Gallenkamp melting point apparatus. The IR spectra were recorded on a Jasco 4100 FT-IR spectrophotometer in KBr discs. The ^{1}H NMR spectra were recorded in $CDCl_3$ and DMSO-d_6 on a Bruker DRX 400 NMR spectrometer operating at 400 MHz for ^{1}H and at 100 MHz for ^{13}C NMR. Chemical shift (δ) values are expressed in parts per million (ppm) and were referenced to the residual solvent signals. The mass spectra were recorded on a Shimadzu GCMS-QP 1000 EX mass spectrometer at 70 eV. Elemental analysis was recorded on a Perkin-Elmer 2400 C,H,N Elemental analyzer; results were in good agreement with calculated values. UV-Vis spectra were performed on

Perkin-Elmer UV/VIS spectrometer lambda 2 with a concentration of 2×10^{-5} M in methanol.

Drugs and chemicals

Iodine-125 was purchased from the Institute of Isotope Co., Ltd. (Budapest), as a carrier-free and reductant-free solution dissolved in diluted NaOH. Methotrexate, PMI 1640 media, Tyrpan blue, *c* (NBS), and sodium metabisulfite were purchased from Sigma Chemical Co., USA. Ehrlich ascites carcinoma (EAC) was supplied from the National Cancer Institute, Cairo, Egypt.

Animals

Female Swiss albino mice weighing 20–25 g were purchased from the Institute of Eye Research Cairo, Egypt. The animals were kept at constant environmental and nutritional conditions throughout the experimental period and kept at room temperature (22 ± 2 °C) with a 12-h on/off light schedule. Female mice were used in this study because of their higher susceptibility to Ehrlich ascites carcinoma. Animals were kept with free access to food and water all over the experiment and were used in this study under the permission of animal rights association in the Egyptian Atomic Authority.

2-(Ethoxycarbonyl)-3-methylquinoxaline 1,4-dioxide (**3**)
A solution of 6.8 g benzofurazan oxide (0.05 mol) and 8 g ethyl acetoacetate (0.06 mol) in 50 cm^3 triethylamine afforded a precipitate after standing at room temperature for 48 h. The precipitate was filtered and recrystallized from acetone-water giving yellow prisms (5.4 g). An additional product fraction (2.6 g) was obtained from the mother liquor after 36 h. Total yield: 8.0 g (65%); m.p.: 133–135 °C (Ref. [10] 132–133 °C).

General procedure for synthesis of arylidine derivatives ***4***

A mixture of 2-(ethoxycarbonyl)-3-methylquinoxaline 1,4-dioxide (**3**, 1 mmol) and aromatic aldehyde (3 mmol) in 1 cm^3 ethanol and a few drops of piperidine were heated at 100 °C in an oil bath for 2 h. After cooling 5 cm^3 ethanol (95%) was added, and the precipitate was filtered and washed with diethyl ether.

(E)-2-(Ethoxycarbonyl)-3-(2-phenylethenyl)quinoxaline 1,4-dioxide (**4a**, $C_{19}H_{16}N_2O_4$)
The separated solid was recrystallized from dimethylformamide and gave the derivative **4a** as yellow crystals (0.32 g, 94%). M.p.: 228–230 °C, IR (KBr): $\bar{\nu}$ = 1736 (CO ester), 1608 (C=C), 1362 (N–O) cm^{-1}; ^{1}H NMR ($CDCl_3$): δ = 1.49 (3H, t, J = 7.2 Hz, CH_3, ester), 4.24 (2H, q, J = 7.2 Hz, CH_2, ester), 6.82–7.55 (5H, m, Phenyl), 6.87(1H, d, J = 16.2 Hz, H_a), 7.76 (2H, m, H-6 and H-7), 8.33 (1H, d, J = 16.2 Hz, H_b), 8.35–8.45 (2H, m, H-5 and H-8) ppm; ^{13}C NMR ($CDCl_3$): δ = 13.71, 62.90, 111.21, 113.24, 113.32 117.45, 117.23, 125.13, 125.89, 128.53, 131.69, 131.55, 131.77, 137.10, 138.99, 145.98, 151.21, 169.53, 171.56 ppm; MS: *m/z* (%) = 336 (M^+, 21.7), 337 (M^++1, 11.2), 320 (M^+–O, 2.2), 304 (M^+–2O, 3.1), 231 ($C_{16}H_{11}N_2$, 13), 128 ($C_8H_4N_2$, 15.5), 104 ($C_6H_4N_2$, 21.7), 77 (C_6H_5, 96.6).

(E)-2-(Ethoxycarbonyl)-3-[2-(4-methoxyphenyl)ethenyl]quinoxaline 1,4-dioxide (**4b**, $C_{20}H_{18}N_2O_5$)
The solid was recrystallized from dimethylformamide and water to give product **4b** as orange crystals (0.28 g, 78%). M.p.: 210–211 °C; IR (KBr): $\bar{\nu}$ = 1736 (CO ester), 1597 (C=C), 1362 (N–O) cm^{-1}; ^{1}H NMR ($CDCl_3$): δ = 1.47 (3H, t, J = 7.2 Hz, CH_3, ester), 3.87 (3H, s, OCH_3), 4.62 (2H, q, J = 7.2 Hz, CH_2, ester), 6.94–7.03 (2H, dd, J = 6.6, 2.1 Hz, phenyl), 6.90 (1H, d, J = 16.2 Hz, H_a), 7.52–7.55 (2H, dd, J = 6.6, 2.1 Hz, phenyl), 7.87 (2H, m, H-6 and H-7), 8.40 (1H, d, J = 16.2 Hz, H_b), 8.58–8.67 (2H, m, H-5 and H-8) ppm; ^{13}C NMR ($CDCl_3$): δ = 13.71, 55.15, 62.90, 114.35, 114.86, 118.77, 118.23, 124.54, 126.13, 126.89, 129.54, 132.62, 132.25, 136.11, 136.99, 139.59, 146.78, 150.21, 170.53, 171.72 ppm; MS: *m/z* (%) = 366 (M^+, 13), 367 (M^++1, 5.2), 365 (18.2), 322 (9.1), 321 (28.6), 320 (14.3), 305 (14.3), 304 (14.3), 303 ($C_{19}H_{15}N_2O_2$, 10.4), 277 ($C_{17}H_{13}N_2O_2$, 16.9), 261 ($C_{17}H_{13}N_2O$, 14.3), 107 ($C_6H_4OCH_3$, 16.9), 104 ($C_6H_4N_2$, 11.7), 77 (C_6H_5, 84.4).

(E)-2-[2-[4-(Dimethylamino)phenyl]ethenyl]-3-(ethoxycarbonyl)quinoxaline 1,4-dioxide (**4c**, $C_{21}H_{21}N_3O_4$)
Red crystals (0.20 g, 53%). M.p.: 221–222 °C (aqueous ethanol); IR (KBr): $\bar{\nu}$ = 1736 (CO ester), 1589 (C=C), 1362 (N–O) cm^{-1}; ^{1}H NMR (DMSO-d_6): δ = 1.37 (3H, t, J = 7.2 Hz, CH_3, ester), 3.00 (6H, s, $N(CH_3)_2$), 4.50 (2H, q, J = 7.2 Hz, CH_2, ester), 6.75–6.77 (2H, d, J = 9 Hz, phenyl), 6.78 (1H, d, J = 15.9 Hz, H_a), 7.46–7.49 (2H, d, J = 9 Hz, phenyl), 7.92–8.00 (2H, m, H-6 and H-7), 8.33 (1H, d, J = 16.2 Hz, H_b), 8.40–8.50 (2H, m, H-5 and H-8) ppm; ^{13}C NMR ($CDCl_3$): δ = 12.70, 44.18, 63.63, 105.22, 111.45, 123.01, 123.21, 124.52, 131.15, 131.53, 132.28, 135.44, 136.23, 137.57, 140.73, 143.00, 160.56 ppm.

(E)-2-[2-[4-(Diethylamino)phenyl]ethenyl]-3-(ethoxycarbonyl)quinoxaline 1,4-dioxide (**4d**, $C_{23}H_{25}N_3O_4$)
Recystallization of the separated solid from aqueous ethanol gave dark red crystals of compound **4d** (0.19 g, 47%). M.p.: 200–202 °C; IR (KBr): $\bar{\nu}$ = 1739 (CO, ester), 1581 (C=C), 1362 (N–O) cm^{-1}; ^{1}H NMR ($CDCl_3$): δ = 1.24 (6H, t, $2CH_3CH_2N$), 1.51 (3H, q, CH_3, ester), 3.45 (4H, q, $2CH_3CH_2N$), 4.63 (2H, q, CH_2, ester),

6.90–6.95 (2H, m, phenyl), 7.52 (1H, d, H_a), 7.53–7.57 (2H, m, phenyl), 7.80–7.88 (2H, m, H-6 and H-7), 8.50 (1H, d, H_b), 8.57–8.66 (2H, m, H-5 and H-8) ppm; ^{13}C NMR ($CDCl_3$): δ = 12.70, 14.18, 44.57, 63.63, 108.22, 111.45, 120.00, 120.27, 122.92, 130.05, 130.55, 132.58, 135.08, 137.67, 138.40, 142.12, 143.44, 160.42 ppm.

(E)-2-(Ethoxycarbonyl)-3-[2-(2-hydroxy-4-nitrophenyl)ethenyl]quinoxaline 1,4-dioxide (**4e**, $C_{19}H_{15}N_3O_7$)

Recystallization of the separated solid from aqueous ethanol gave dark red crystals of compound **4e** (0.25 g, 62%). M.p.: 190–191 °C; IR (KBr): $\bar{\nu}$ = 1743 (CO, ester), 1597 (C=C), 1350 (N–O) cm^{-1}; ^{1}H NMR ($CDCl_3$): δ = 1.47 (3H, t, CH_3, ester), 1.90 (1H, s, OH), 4.63 (2H, q, CH_2, ester), 6.90 (1H, m, phenyl), 7.42 (1H, d, H_a), 7.52–7.55 (2H, m, phenyl), 7.90–8.00 (2H, m, H-6 and H-7), 8.20 (1H, d, H_b), 8.58–8.69 (2H, m, H-5 and H-8) ppm; ^{13}C NMR ($CDCl_3$): δ = 14.71, 63.98, 114.21, 116.24, 125.69, 128.33, 131.09, 131.75, 131.77, 133.32 133.45, 137.10, 138.99, 145.98, 149.23, 150.21, 160.13, 168.54, 171.88 ppm.

(E)-2-[2-(Dimethylamino)ethenyl]-3-(ethoxycarbonyl)quinoxaline 1,4-dioxide (**5**, $C_{15}H_{17}N_3O_4$)

A mixture of 0.248 g 2-(ethoxycarbonyl)-3-methylquinoxaline 1,4-dioxide (**3**, 0.01 mol) and 1.79 g DMF-DMA (0.015 mol) in 20 cm^3 benzene was refluxed for 24 h. The solvent was removed under reduced pressure, and the red precipitate was triturated with diethyl ether to give **5** (2.36 g, 78%). M.p.: 158–160 °C; IR (KBr): $\bar{\nu}$ = 1739 (CO), 1593 (C=C), 1364 (N–O) cm^{-1}; ^{1}H NMR ($CDCl_3$): δ = 1.47 (3H, t, J = 7.2 Hz, CH_3CH_2), 3.02 (6H, s, $N(CH_3)_2$), 4.59 (2H, q, J = 7.2 Hz, CH_2CH_3), 4.76 (1H, d, J = 15.5 Hz, H_b), 7.57–7.81 (2H, m, H-6 and H-7), 8.45–8.49 (2H, m, H-5 and H-8), 9.57 (1H, d, J = 15.5 Hz, H_a) ppm; ^{13}C NMR ($CDCl_3$): δ = 14.13, 63.22, 84.12, 119.37, 120.88, 132.40, 133.77, 136.21, 137.17, 137.95, 138.17, 136.55, 151.29, 160.95 ppm; MS: *m/z* (%) = 303 (M^+, 23.3), 304 (M^++1, 10.0), 287 (M^+–O, 8.3), 198 ($C_{12}H_{12}N_3$, 46.7), 184 ($C_{10}H_6N_3O$, 15.0), 168 ($C_{10}H_6N_3$, 16.7), 128 ($C_8H_4N_2$, 41.7), 104 ($C_6H_4N_2$, 41.7).

(E)-2-(Ethoxycarbonyl)-3-[2-(4-morpholinyl)ethenyl]quinoxaline 1,4-dioxide (**6**, $C_{17}H_{19}N_3O_5$)

A mixture of 0.3 g enamine **5** (1 mmol) and 0.78 g morpholine (1 mmol) in 10 cm^3 chloroform and 10 cm^3 isopropanol in presence of 0.12 g *p*-toluenesulfonic acid (1 mmol) was refluxed for 6 h. The solvent was reduced to half of its volume, and the formed precipitate was filtered off. The filtrate was poured on cold water and extracted with chloroform to get an additional amount of product **6**. The product was purified by column chromatography using 2% ethanol/dichloromethane as eluent to give compound **6** (0.27 g, 80%). M.p.: 162–164 °C; IR (KBr): $\bar{\nu}$ = 1743 (CO), 1589 (C=C), 1358 (N–O) cm^{-1}; ^{1}H NMR ($CDCl_3$): δ = 1.47 (3H, t, J = 7.4 Hz, CH_3), 3.34 (4H, t, J = 5.4 Hz, CH_2NCH_2), 3.76 (4H, t, J = 5.3 Hz, CH_2OCH_2), 4.57 (2H, t, J = 7.2 Hz, CH_2CH_3), 4.97 (1H, d, J = 15.3 Hz, H_b), 7.60–7.86 (2H, m, H-6 and H-7), 8.46–8.50 (2H, m, H-5 and H-8), 9.49 (1H, d, J = 15.3 Hz, H_a) ppm; ^{13}C NMR ($CDCl_3$): δ = 14.45, 54.66, 63.22, 66.87, 85.62, 129.32, 121.34, 131.43, 131.72, 136.21, 136.47, 138.05, 138.55, 135.64, 150.89, 160.81 ppm; MS: *m/z* (%) = 329 (M^+–O, 3.8), 239 ($C_{14}H_{13}N_3O$, 34.6), 129 ($C_8H_5N_2$, 51.9).

General procedure for synthesis of pyrido[3,4-b]quinoxaline 5,10-dioxides ***8***

A solution of enamine **5** (1 mmol) and an aliphatic amine (1 mmol) in 10 cm^3 chloroform and 10 cm^3 isopropanol in the presence of 0.12 g *p*-toluenesulfonic acid (1 mmol) was refluxed for 4–8 h. The solvent was reduced to half of its volume, and the precipitate was filtered off to give a crude product. The filtrate was poured on cold water and extracted with chloroform to afford a further amount of product. The combined product was purified by column chromatography using 2% ethanol/dichloromethane as eluent.

1,2-Dihydro-2-methyl-1-oxopyrido[3,4-b]quinoxaline 5,10-dioxide (**8a**, $C_{12}H_9N_3O_3$)

Yield 0.16 g (67%); m.p.: 164–166 °C; IR (KBr): $\bar{\nu}$ = 3097 (=CH), 1670 (CO), 1620 (C=C), 1346 (N–O) cm^{-1}; ^{1}H NMR ($CDCl_3$): δ = 3.71 (3H, t, CH_3), 7.27–7.38 (2H, m, H-6 and H-7), 7.83–7.86 (2H, m, H-5 and H-8), 8.44 (1H, d, J = 9.3 Hz, H_b), 8.62 (1H, d, J = 9.3 Hz, H_a) ppm; ^{13}C NMR ($CDCl_3$): δ = 32.49, 127.87, 128.99, 131.84, 132.69, 132.01, 134.39, 135.54, 137.31, 141.31, 145.00, 160.47 ppm; MS: *m/z* (%) = 227 (M^+–O, 39.1), 211 (M^+–2O, 8.3), 141 ($C_9H_5N_2$, 7.5), 128 ($C_8H_4N_2$, 2.3).

1,2-Dihydro-1-oxo-2-(phenylmethyl)pyrido[3,4-b]quinoxaline 5,10-dioxide (**8b**, $C_{18}H_{13}N_3O_3$)

Yield 0.21 g (66%); m.p.: 206–207 °C; IR (KBr): $\bar{\nu}$ = 1678 (CO), 1608 (C=C), 1340 (N–O) cm^{-1}; ^{1}H NMR ($CDCl_3$): δ = 5.30 (2H, s, CH_2Ph), 7.27–7.38 (5H, m, Phenyl), 7.39–7.42 (2H, m, H-6 and H-7), 7.84–7.88 (2H, m, H-5 and H-8), 8.44 (1H, d, J = 9.3 Hz, H_b), 8.61 (1H, d, J = 9.3 Hz, H_a) ppm; ^{13}C NMR ($CDCl_3$): δ = 52.49, 96.51, 118.76, 128.60, 129.22, 131.50, 132.15, 132.51, 135.34, 135.66, 137.21, 140.32, 144.21, 160.77 ppm; MS: *m/z* (%) = 303 (M^+-O, 12.4), 168 ($C_{10}H_6N_3$, 2.2), 128 ($C_8H_4N_2$, 3.4), 91 ($C_6H_4CH_3$, 100).

2-Butyl-1,2-dihydro-1-oxopyrido[3,4-b]quinoxaline 5,10-dioxide (**8c**, $C_{15}H_{15}N_3O_3$)

Yield 0.19 g (68%); m.p.: 225–226 °C; IR (KBr): $\bar{\nu}$ = 1670 (CO), 1612 (C=C), 1340 (N–O) cm^{-1}; ^{1}H

NMR ($CDCl_3$): $\delta = 1.00$ (3H, t, $J = 7.3$ Hz, CH_3), 1.45 (2H, m, CH_3CH_2), 1.82 (2H, quint, $CH_2CH_2CH_2$), 4.10 (2H, t, $J = 7.3$ Hz, CH_2N), 7.27–7.29 (2H, m, H-6 and H-7), 7.84–7.87 (2H, m, H-5 and H-8), 8.43 (1H, d, $J = 9.3$ Hz, H_b), 8.62 (1H, d, $J = 9.3$ Hz, H_a) ppm; ^{13}C NMR ($CDCl_3$): $\delta = 13.84$, 20.00, 31.14, 50.01, 116.75, 120.11, 131.89, 137.94, 138.55, 140.45, 144.54, 146.48, 147.37, 160.16 ppm; MS: *m/z* (%) = 269 (M^+–O, 42.4), 253 (M^+–2O, 41.2), 212 ($C_{11}H_6N_3O_2$, 20.0), 184 ($C_{10}H_6N_3O$, 14.1), 168 ($C_{10}H_6N_3$, 34.1), 141 ($C_9H_5N_2$, 41.2), 128 ($C_8H_4N_2$, 11.8).

1,2-Dihydro-1-oxo-2-phenylpyrido[3,4-b]quinoxaline 5,10-dioxide (**8d**, $C_{17}H_{11}N_3O_3$)
Yield 0.24 g (80%); m.p.: 237–238 °C; IR (KBr): $\bar{\nu} = 1674$ (CO), 1616 (C=C), 1335 (N–O) cm^{-1}; ^1H NMR ($CDCl_3$): $\delta = 7.27$–7.55 (5H, m, phenyl), 7.57–7.60 (2H, m, H-6 and H-7), 7.87–7.90 (2H, m, H-5 and H-8), 8.44 (1H, d, $J = 9.3$ Hz, H_b), 8.61 (1H, d, $J = 9.3$ Hz, H_a) ppm; ^{13}C NMR ($CDCl_3$): $\delta = 96.19$, 118.80, 126.30, 130.38, 131.50, 132.22, 132.60, 136.70, 139.13, 140.67, 144.27, 160.37 ppm; MS: *m/z* (%) = 289 (M^+–O, 11.4), 273 (M^+–2O, 7.2), 104 ($C_6H_4N_2$, 14.8), 77 (C_6H_5, 100).

1,2-Dihydro-2-(4-methylphenyl)-1-oxopyrido[3,4-b]-quinoxaline 5,10-dioxide (**8e**, $C_{18}H_{13}N_3O_3$)
Yield 0.25 g (78%); m.p.: 236–237 °C; IR (KBr): $\bar{\nu} = 1678$ (CO), 1608 (C=C), 1346 (N–O) cm^{-1}; ^1H NMR ($CDCl_3$): $\delta = 2.45$ (3H, s, CH_3), 7.35–7.39 (4H, m, phenyl), 7.45–7.48 (2H, m, H-6 and H-7), 7.86–7.89 (2H, m, H-5 and H-8), 8.45 (1H, d, $J = 9.3$ Hz, H_b), 8.63 (1H, d, $J = 9.3$ Hz, H_a) ppm; ^{13}C NMR ($CDCl_3$): $\delta = 21.35$, 96.19, 118.89, 126.30, 130.38, 131.50, 132.22, 132.60, 136.70, 139.13, 140.67, 144.27, 160.37 ppm; MS: *m/z* (%) = 303 (M^+-O, 38.1), 287 (M^+–2O, 22.7), 128 ($C_8H_4N_2$, 10.3), 91 ($C_6H_4CH_3$, 100), 77 (C_6H_5, 40.2).

Labeling procedure and requirement

Iodo-AVQD was prepared by electrophilic substitution of H_b with iodonium ion using NBS as oxidizing agent [23]. AVQD (1 mg, 3.3 µmol) was dissolved in 1 cm^3 DMF, and 10 mm^3 of this solution was transferred to a colored vial. The pH was adjusted to pH = 9 with 0.5 M phosphate buffer pH 9. A solution (2.5 mm^3, 1.4 µmol NBS) of 10 mg NBS (56 µmol) in 100 mm^3 distilled water was added to the AVQD solution, followed by the addition of approximately 18–37 MBq (0.5–1 µCi) carrier free $Na^{125}I$ at room temperature. Total volume was adjusted to 250 mm^3 with 0.5 M phosphate buffer, pH 9. After 5 min, the reaction was stopped using 0.2 N sodium metabisulfite solutions (100 mm^3) to ensure that the unreacted iodine was reduced before chromatographic analysis [23]. The yield of the reaction and the radiochemical purity were determined by paper electrophoresis and thin layer chromatography.

Electrophoresis conditions

Electrophoresis was done with an EC 3000 p-series 90 programmable power and chamber supply unit using cellulose acetate strips (45 cm). These strips were moistened with 0.05 M phosphate buffer, pH 7, and then introduced in the chamber. Samples were applied at a distance of 10 cm from the cathode. Standing time and applied voltage were continued for 1.5 h. Developed strips were dried and cut into 1-cm segments, then counted by a well-type NaI scintillation counter. The radiochemical yield was calculated as the ratio of the radioactivity of the labeled product to the total radioactivity [28].

Thin layer chromatography

Thin layer chromatography was achieved using chloroform:ethanol:ammonia (90:10:0.05) as mobile phase and TLC plates covered with Silica Gel G-60. The R_f value was about 0.9 for ^{125}I- AVQD, while free iodide resisted at the point of spotting [23].

In vitro stability

This experiment was conducted to determine the stability of ^{125}I-AVQD after labeling and the impact of time on that compound. The yield was measured at different time intervals: 1, 4, 12, 24, and 48 h after labeling.

Induction of solid tumor in mice

The parent tumor line (Ehrlich Ascites Carcinoma) was withdrawn from 7-day-old downer female Swiss albino mice and diluted with sterile physiological saline solution to give 12.5 × 10^6 cells/cm^3. An aliquot of 0.2 cm^3 solution was then injected in each mouse intramuscularly in the right thigh to produce solid tumor [29].

In vivo biodistribution

In normal mice
In vivo biodistribution studies were performed using four groups of six mice each. Each animal was injected in the tail vein with 0.2 cm^3 solution containing 5–10 kBq of ^{125}I-AVQD. The mice were kept in metabolic cages for the required time. Each group was subjected to scarification by cervical dislocation at the recommended time (15 min, 1,

4, or 24 h) after injection. Organs or tissues of interest were removed, washed with saline, weighed, and counted. Correction was made for background radiation and physical decay during the experiment [24]. The weights of blood, bone, and muscles were assumed to be 7, 10, and 40% of the total body weight, respectively [30].

In solid tumor-bearing mice

Biodistribution of ^{125}I-AVQD was carried out in a group consisting of 24 solid tumor-bearing mice as mentioned for normal mice. Left and right legs were removed and counted. Normal and tumor muscles were removed, weighed, and counted. The tumor to non-tumor ratio was calculated (target to non-target ratio). The results were calculated as percentages of injected dose (I.D.) per gram tissue. The final results were expressed as mean ± 1 standard error [31].

Radiotoxicity of ^{125}I-AVQD on Ehrlich cells

This experiment was performed by mixing a set of sterile test tubes containing 0.1 cm^3 of tumor cell suspension, 0.8 cm^3 RPMI 1640 media, and different concentrations of ^{125}I-AVQD. The test tubes were incubated at 37 °C in a titanox incubator for 2 h. Then the tubes were centrifuged (Harmonic centrifuge), and the cells were separated by aspiration of the supernatant and stained with trypan blue. The percentage of nonviable cells (NVC) was calculated using a haemocytometer [32].

Statistical analysis

The results were expressed as means ± SEM for the indicated number of different experiments. To compare the difference among the groups, an unpaired Student's test was performed. A p value of less than 0.05 was considered significant.

References

1. Zarranz B, Jaso A, Aldana I, Monge A (2004) Bioorg Med Chem 12:3711
2. Denny WA, Wilson WR (1986) J Med Chem 29:879
3. Overgaad J (1992) Radiother Oncol 24:564
4. Fuchs T, Chowdhury G, Barnes CL, Gates KS (2001) J Org Chem 66:107
5. Villa MA (2001) Radiobiologia 1:7
6. Brown JM, Koong AJ (1999) J Natl Cancer Inst 83:178
7. Ibrahim IT, Wally MA (2009) J Radioanal Nucl Chem. doi: 101007/s10967-009-0039-1
8. Benson AB III, Trump DL, Cummings KB, Fischer PH (1985) Biochem Pharmacol 34:3925
9. Mester J, DeGoeij K, Sluyser M (1996) Eur J Cancer 32A:1603
10. Unak T (2000) Curr Pharm 11:1127
11. Walicka MA, Adelstein SJ, Kassis AI (1998) Radiat Res 149:134
12. Monge A, Palop JA, López de Cerain A, Senador V, Martinez-Crespo FJ, Sainz Y, Narro S, Garcia E, de Miguel C, Gonzalez M, Hamilton E, Barker AJ, Clarke ED, Greenhow DT (1995) J Med Chem 38:1786
13. Chowdhury G, Kotandeniya D, Daniels JS, Barnes CL, Gates KS (2004) Chem Res Toxicol 17:1399
14. Fuchs T, Gates KS, Hwang J-T, Greenberg MM (1999) Chem Res Toxicol 12:1190
15. Sternberg ED, Dolphin D, Bruckner C (1998) Tetrahedron 54:4151
16. Dolphin D (1994) Cancer J Chem 72:1005
17. Rouhl AM (1998) Chem Eng News 76:22
18. Doughery TJ (1987) Photochem Photobiol 45:879
19. Miller J (1999) J Chem Ed 76:592
20. Issidorides CH, Haddadin MJ (1966) J Org Chem 31:4067
21. Haddadin MJ, Issidorides CH (1993) Heterocycles 35:1503
22. Lyubchanskaya VM, Alekseeva LM, Granik VG (1992) Chem Heterocycl Comp 28:34
23. Chi KH, Wang HE, Chen FD (2001) J Nucl Med 42:345
24. Kassis AI, Sastry KSR, Adelestein SJ (1987) Radiat Res 109:78
25. Montgomery J (1970) Med Chem 3:680
26. Harrison KA, Dalrymple GV, Baranowska-Kortylewicz J (1996) J Nucl Med 37:13S
27. Kassis AI, Tumeh SS, Wen PY (1996) J Nucl Med 37:19S
28. Hofer KG, Van Loon N, Schnederman MH, Charlton DE (1992) Radiat Res 130:121
29. Klecker RW Jr, Jenkins JF, Kinsella TJ, Fine RL, Strong JM, Clin JM (1985) Pharmacol Ther 38:45
30. El-Ghany EA, Mahdy MA, Attallah K, Ghazy FS (2002) J Radioanal Nucl Chem 1:156
31. El-Ghany EA, Mahdy MA, Attallah K, Ghazy FS (2004) Arab J Nucl Sci Appl 37:1
32. Desombre ER (1992) Cancer Res 52:5752